Supporting Information

Low Band Gap π-conjugated Porous Polymers as Bifunctional Photoelectrocatalysts for Overall Water Splitting

Bantumelli Prachuritha,[a] Pranav Utpalla,[a] Dasari Sai Hemanth Kumar,[a] and Krishnamurthi Muralidharan*[a]

[*]*School of Chemistry, University of Hyderabad, Hyderabad, 500046, India*

Corresponding author: *murali@uohyd.ac.in*

Table of Contents	**Page No.**
TRPL decay parameters (Table S1)	2
Average particle size of PDM2:1, PDM1:2, and PDM1:1 respectively (Fig. S1)	2
Electrochemical Bandgap calculation of PDMD2:1, PDM1:2, and PDM1:1 respectively using cyclic voltammetry (Fig. S2)	2
Experimentally calculated HOMO LUMO energy levels (Table S2)	2
Comparison table showing OER overpotential values (mV at η_{10}) in reported literature (Table S3)	3
Estimation of electrochemical surface area (ECSA) & CV plots at different scan rates (20 – 100 mV s^{-1}) for HER studies (Fig. S3)	3
LSV plots (OER) before & after chronoamperometry (Fig. S4)	4
LSV stability (500 cycles) (Fig. S5)	5
Microscopic analysis of electrodes after 500 cycles of stability (Fig. S6)	
Microscopic analysis of post-chronoamperometric electrolysis electrode (Fig. S7)	5
Faradaic efficiency calculation & Photographic/videographic illustration of photoelectrochemical setup (Fig. S8)	5
Comparison table showing HER overpotential values (mV at η_{10}) in reported literature (Table S4)	6
Estimation of electrochemical surface area (ECSA) & CV plots at different scan rates (20 – 100 mV s^{-1}) for HER studies (Fig. S9)	7
LSV plots (HER) before & after chronoamperometry (Fig. S10)	7
Microscopic analysis of post-chronoamperometric electrolysis electrode (Fig. S11)	7
Gas Analysis in Overall Water Splitting (Fig. S12)	8
Microscopic analysis of post-chronoamperometric electrolysis electrode (OWS) (Fig. S13)	8
EIS fit results (Table S5)	9
M-S slope values (Table S6)	9
M-S plots (Fig. S14)	9
Prototype showing bulk electrolysis for overall water splitting (Fig. S15)	9
References	10

Average particle size of the polymers PDM1:1, PDM1:2, and PDM2:1

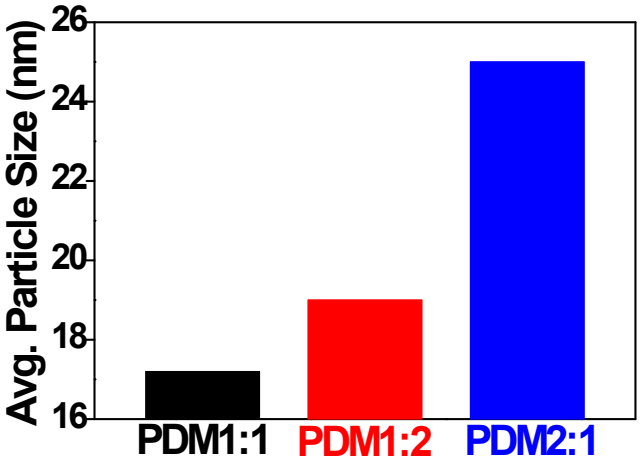

Fig. S1. *Average particle size of PDM2:1, PDM1:2, and PDM1:1, respectively (Calculated from TEM images using ImageJ software).*

Table S1. TRPL decay parameters.

Polymer	τ_s (ns)	τ_i (ns)	τ_l (ns)	B_s	B_i	B_l	τ_{avg} (ns)	χ^2
PDM2:1	0.511	0.787	4.442	683387.6	34978.9	573.3	0.6	1.05
PDM1:1	0.419	1.559	5.06	34734.5	15959.4	4123.4	1.1	1.18
PDM1:2	0.571	2.656	3.092	14806.1	125266.2	191578.6	1.3	1.16

The data was fitted using the triexponential function: $A + B_s e^{(-t/\tau_s)} + B_i e^{(-t/\tau_i)} + B_l e^{(-t/\tau_l)}$
'*A*' is the constant term, 'B_s', 'B_i', and 'B_l' are the pre-exponential factor (amplitude) corresponding to decay lifetimes: shorter lifetime-- τ_s, intermediate lifetime-- τ_i, and longer lifetime-- τ_l, respectively. τ_{avg} is the average lifetime calculated by $\tau_{avg} = \{(B_s \tau_s) + (B_i \tau_i) + (B_l \tau_l)\}/(B_s+B_i+B_l)$

Bandgap calculation using cyclic voltammetry

Following the reported literature S1, the higher occupied molecular orbital (HOMO) and lowest unoccupied molecular orbital (LUMO) energy levels were calculated using ferrocene reference system. To determine the experimental HOMO and LUMO values in eV units, the following formulae were used.[S2]

$$E_{HOMO} = -e\left(E_{OX}^{ONSET} + 4.4\right)$$

$$E_{LUMO} = -e(E_{RED}^{ONSET} + 4.4)$$

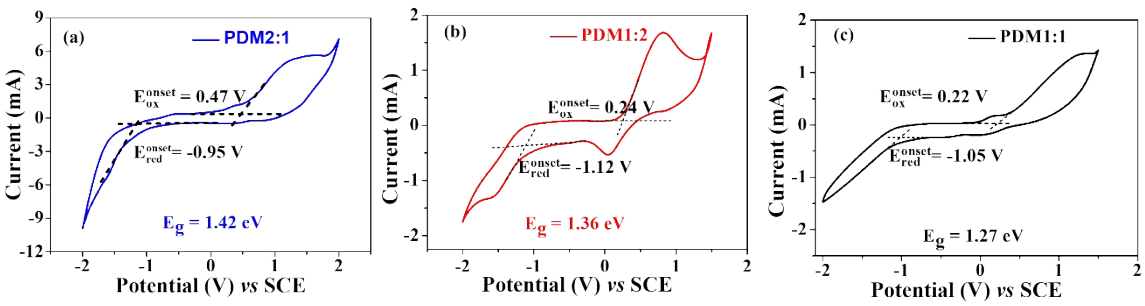

Fig. S2. (*a, b, c) Cyclic voltammograms of PDM2:1, PDM1:2, and PDM1:1 showing onset oxidation and reduction potential, respectively.*

Table S2. *Experimentally calculated HOMO-LUMO energy levels of PDM2:1, PDM1:2, and PDM1:1 w.r.t. SCE.*

Polymer	HOMO (eV)	LUMO (eV)	E_g (eV)
P2:1	-4.87	-3.45	1.42
P1:2	-4.64	-3.28	1.36
P1:1	-4.62	-3.35	1.27

Electrochemical Studies (OER)

Table S3. *Comparison table showing overpotential values (mV @ η_{10}) towards OER in the reported literature.*

Catalyst	Overpotential (mV at η_{10})	Reference
Nitrogen-doped carbon materials	380	[S3]
Acidic oxidation of commercially available carbon cloth (CC)	328	[S4]
PEMAc@CNTs90	298	[S5]
Co^{2+} - containing phthalocyanine-based porous conjugated organic polymer	340	[S6]
CoP nanoparticles, which are encapsulated by a biomolecule-derived N, P-codoped carbon nanosheets	310	[S7]
Co-MPPy-1	420	[S7]
Co/b-Mo2C@N-CNTs	356	[S8]
Ni(II)-based CP $[Ni(MCA)(bipy)(H_2O)_2]_n$	530	[S9]
Porphyrin-conjugated microporous polymer (CMP)	370	[S10]
Electrodeposited Co-P films	345	[S11]
Cobalt-based MOFs	319	[S12]
Melamine-pyrrole-based CMP	**240 (dark)** **230 (illumination)**	**Present Work**

Estimation of electrochemical surface area (ECSA)

The electrochemical surface area (ECSA) was determined by recording cyclic voltammograms at different scan rates (Fig. *S3*) through the estimation of double-layer capacitance (C_{dl}).

ECSA was calculated as follows:
Double-layer capacitance (C_{dl}) (F cm^{-2}) = slope of the plot Δj (mA cm^{-2}) *vs* scan rate (mV s^{-1})
Geometrical surface area of electrode used = 0.8 x 0.5 cm^2
C_{dl} (F) = C_{dl} (F cm^{-2}) x electrode surface area (cm^2)
C_s of nickel foam[S13] = 40 µF cm^{-2}
ECSA (cm^2) = C_{dl} (F) / C_s (F cm^{-2})

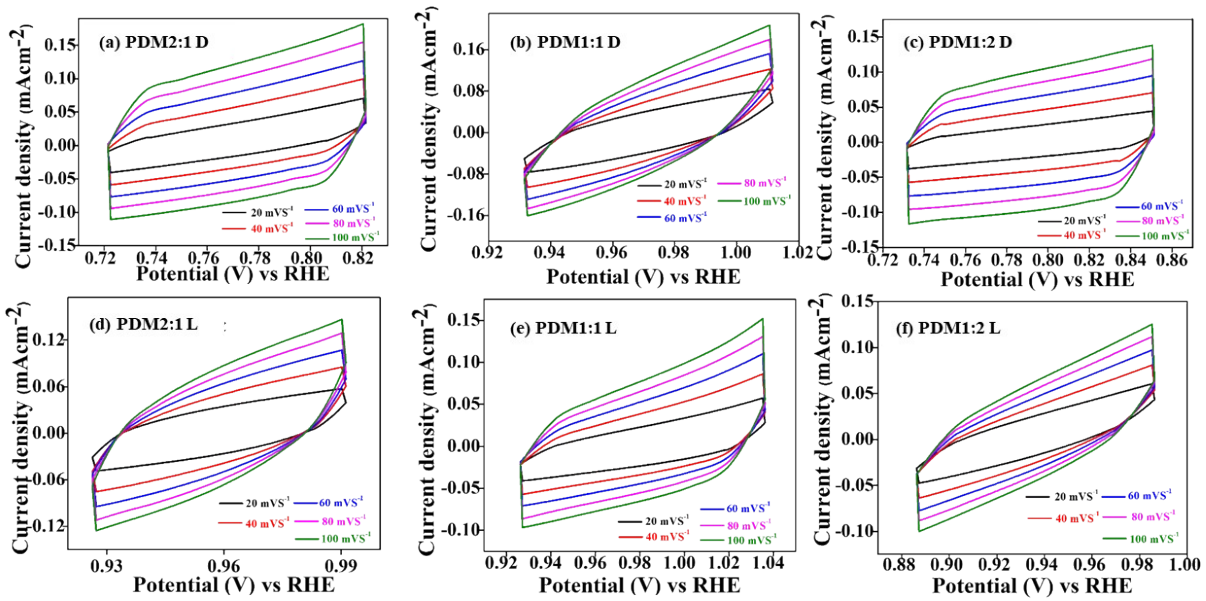

Fig. S3. *Cyclic voltammograms at different scan rates (20 – 100 mV s^{-1}): **(a-c)** CV plots of polymers PDM2:1, PDM1:1, and PDM1:2 under dark conditions **(d-f)** CV plots of polymers PDM2:1, PDM1:1, and PDM1:2 under illumination conditions, respectively.*

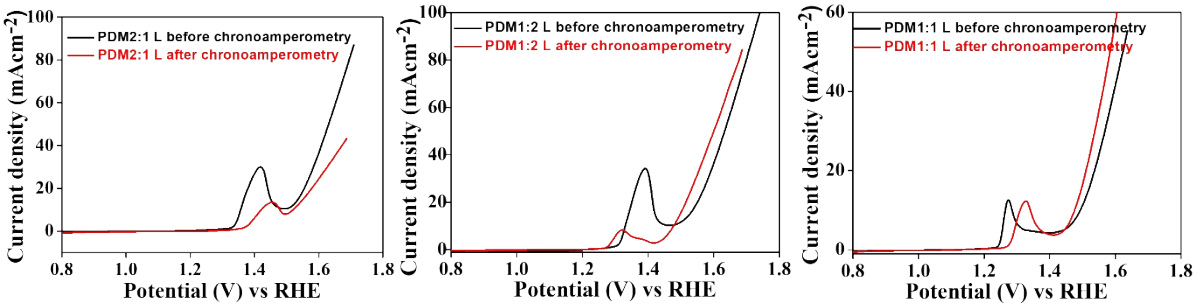

Fig. S4. *LSV plots of the polymers PDM2:1, PDM1:2, and PDM1:1 before and after chronoamperometry for 24 h under illumination conditions.*

LSV stability (500 cycles)

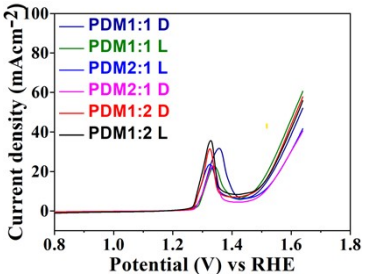

Fig. S5. *Linear sweep voltammograms of polymers PDM2:1, PDM1:1, and PDM1:2 under dark & illumination conditions, respectively, after 500 cycles of CV.*

Microscopic analysis of photocatalyst coated electrode after CV 500 cycles

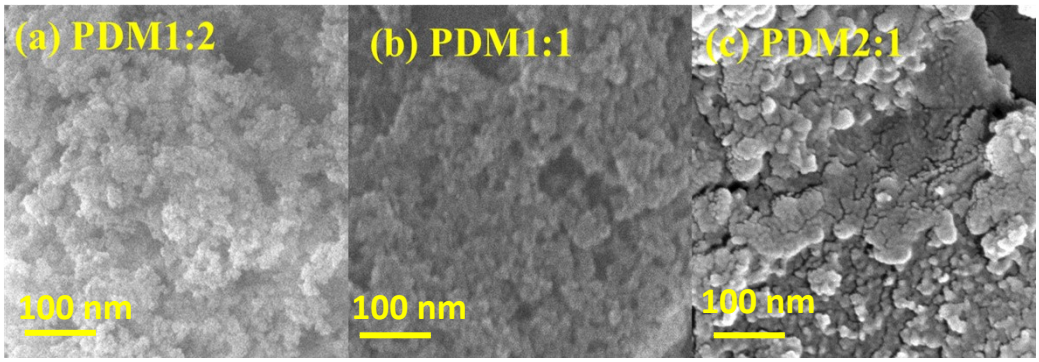

Fig. S6. *FESEM images of electrodes after CV 500 cycles, (a-c) PDM1:2, PDM1:1, and PDM2:1, respectively.*

Microscopic analysis of photocatalyst coated electrode post chronoamperometry

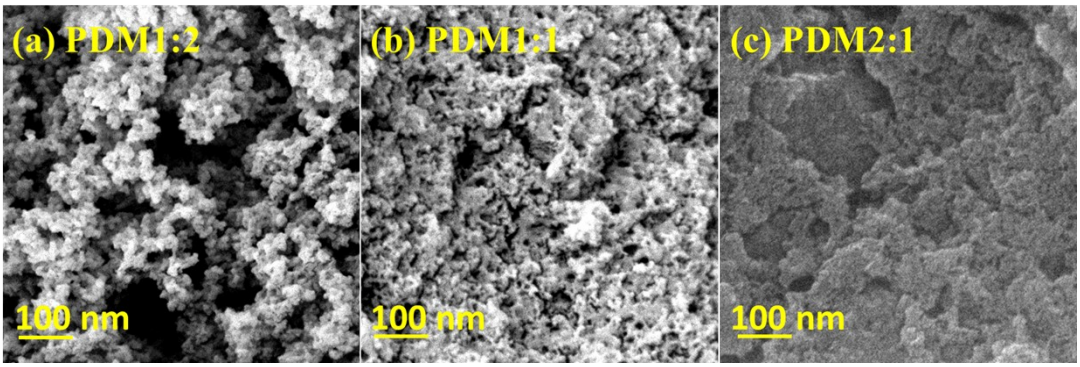

Fig. S7. *FESEM images of post-chronoamperometric electrolysis electrodes, PDM1:2, PDM1:1, and PDM2:1, respectively.*

Faradaic efficiency calculation

As per the reported literature [14], faradaic efficiency of the catalysts was determined under dark and illuminated conditions using a two-electrode system (working and counter electrode). Active material drop cast on nickel foam was a working electrode and platinum wire was used as a counter electrode. The oxygen gas evolved at a constant current (20 mA) over time (1 h) was measured. Photographic/videographic illustration of the OER bulk electrolysis is shown in Fig. S7 a&b.

Under dark conditions, the oxygen gas evolved at a constant current over 1 h duration and was found to be 3.8, 3.6, and 2.6 mL for PDM1:2, PDM1:1, and PDM2:1 polymer, respectively. While, under illumination conditions, it was found to be 4.0, 3.75, and 2.95 mL for PDM1:2, PDM1:1, and PDM2:1 polymer, respectively. Therefore, faradaic efficiency was calculated as follows.

Detailed calculation is given for PDM1:2 polymer under illumination conditions:

No. of moles of oxygen gas evolved in 1 h = 4.0 mL/ 22400 mL.mol^{-1} = 17.8 x 10 $^{-5}$ mol

$$O_2\ (ideal) = \frac{Q}{n \times F}$$

Where *Q* is total charge employed, *n* is no. of electrons required for a chemical change, and *F* is Faraday constant.

O_2 ideal = 0.02 x 3600 / 4 x 96500 = 18.653 x 10 $^{-5}$ mol

% *FE* = (17.8 x 10 $^{-5}$ / 18.653 x 10 $^{-5}$) x 100

= 95.4 %

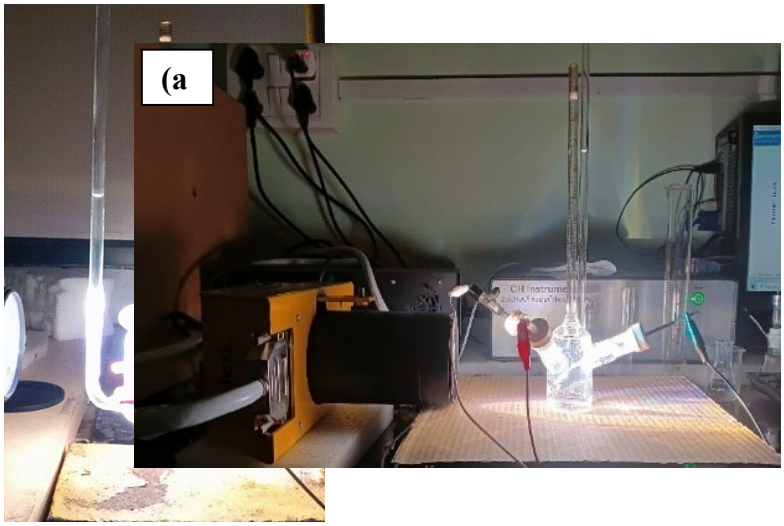

Fig. S8. *(a & b) Photographic/videographic illustration of OER bulk electrolysis by CMP photoelectrocatalyst*

Electrochemical studies (HER)

Table S4. *Comparison table showing overpotential values (mV at η_{10}) towards HER in the reported literature.*

Catalyst	**Overpotential (mV at η_{10})**	**Reference**
Py-DPABT CMP	325	[S15]
FP-950	299	[S16]
Ni-POR-Py Cu-POR-Py	213 250	[S17]
metallocorrole	860	[S18]
N-doped graphene	474	[S19]
nanoporous-graphene	650	[S20]
C_3N_4/N-doped graphene mixture	380	[S21]
N, P-doped carbon (SA900)	419	[S22]
2D conjugated COFs (2DCCOF1)	541	[S23]
Metal-coordinated Bpy-based CMP	285	[S24]
Melamine-pyrrole-based CMP	252 (dark) 229 (illumination)	Present Work

Estimation of electrochemical surface area (ECSA)

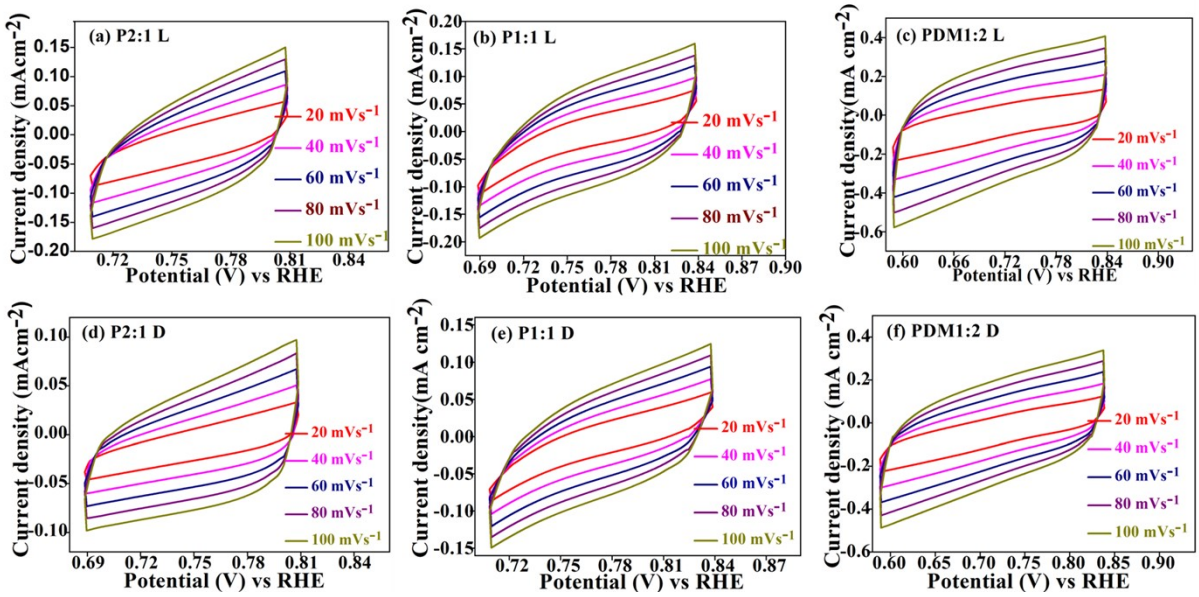

Fig. S9 *Cyclic voltammograms at different scan rates (20 – 100 mV s^{-1}):* ***(a-c)*** *CV plots of polymers PDM2:1, PDM1:1, and PDM1:2 under illuminated conditions, respectively.* ***(d-f)*** *CV plots of the polymers PDM2:1, PDM1:1, and PDM1:2 under dark conditions.*

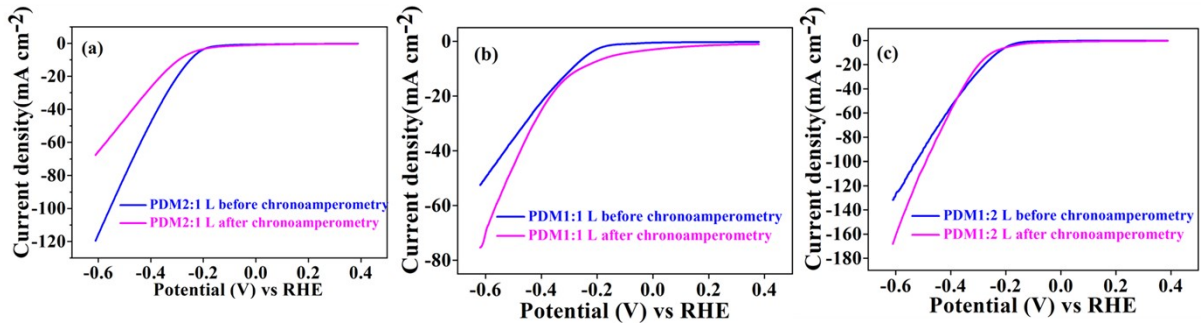

Fig. S10. (a-c) *LSV plots of the polymers PDM2:1, PDM1:2, and PDM1:1 before and after chronoamperometry for 24 h under illumination conditions.*

Microscopic analysis of the electrode post-chronoamperometric electrolysis

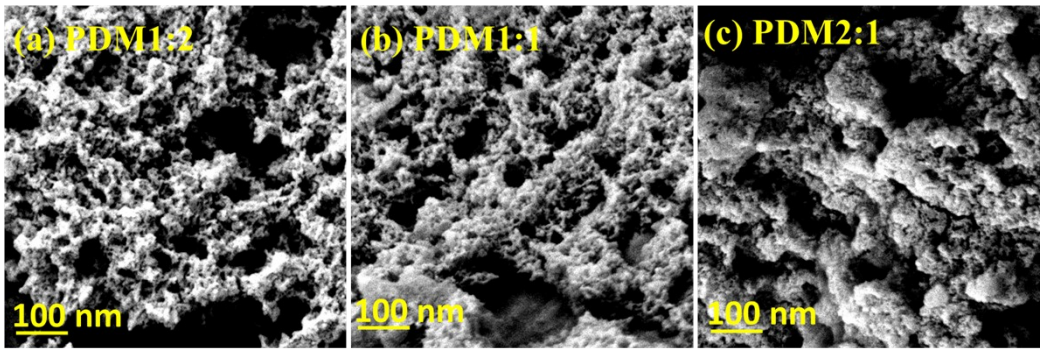

Fig. S11. *FESEM images of post-chronoamperometric electrolysis electrodes, PDM1:2, PDM1:1, and PDM2:1, respectively.*

Gas Analysis in Overall Water Splitting

Gas Chromatography (GC) analysis confirms the presence of both hydrogen and oxygen gases, as shown below. However, the optimal 2:1 molar ratio or peak area for H_2:O_2 is not observed because H_2 has much higher thermal conductivity and thus very high "*Relative Response Factor*" than O_2 in Thermal Conductivity Detector used here. Hence, H_2 peak area is disproportionately larger than O_2 because the detector is more sensitive to H_2. Other reasons for less O_2 peak area might be due to more solubility of O_2 compared to H_2 in water so O_2 may stay dissolved in electrolyte or oxygen consumption for surface oxidation of electrode, etc.

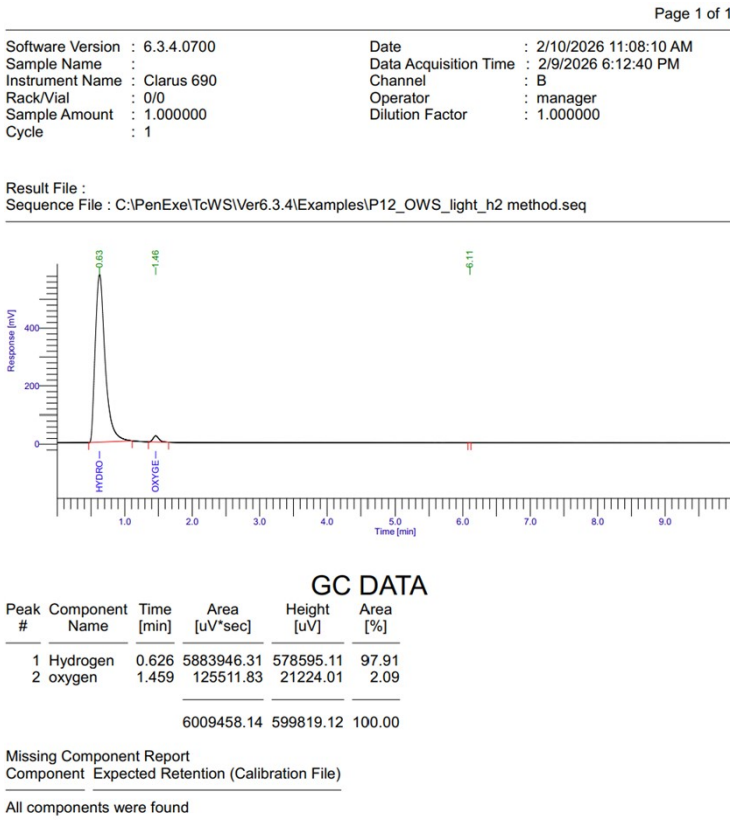

Page 1 of 1

Software Version	: 6.3.4.0700	Date	: 2/10/2026 11:08:10 AM
Sample Name	:	Data Acquisition Time	: 2/9/2026 6:12:40 PM
Instrument Name	: Clarus 690	Channel	: B
Rack/Vial	: 0/0	Operator	: manager
Sample Amount	: 1.000000	Dilution Factor	: 1.000000
Cycle	: 1		

Result File :
Sequence File : C:\PenExe\TcWS\Ver6.3.4\Examples\P12_OWS_light_h2 method.seq

GC DATA

Peak #	Component Name	Time [min]	Area [uV*sec]	Height [uV]	Area [%]
1	Hydrogen	0.626	5883946.31	578595.11	97.91
2	oxygen	1.459	125511.83	21224.01	2.09
			6009458.14	599819.12	100.00

Missing Component Report

Component	Expected Retention (Calibration File)

All components were found

Fig. S12. *Gas chromatographic analysis report for polymer PDM1:2.*

Electrochemical studies (OWS)

Microscopic analysis of post-chronoamperometric electrolysis electrode

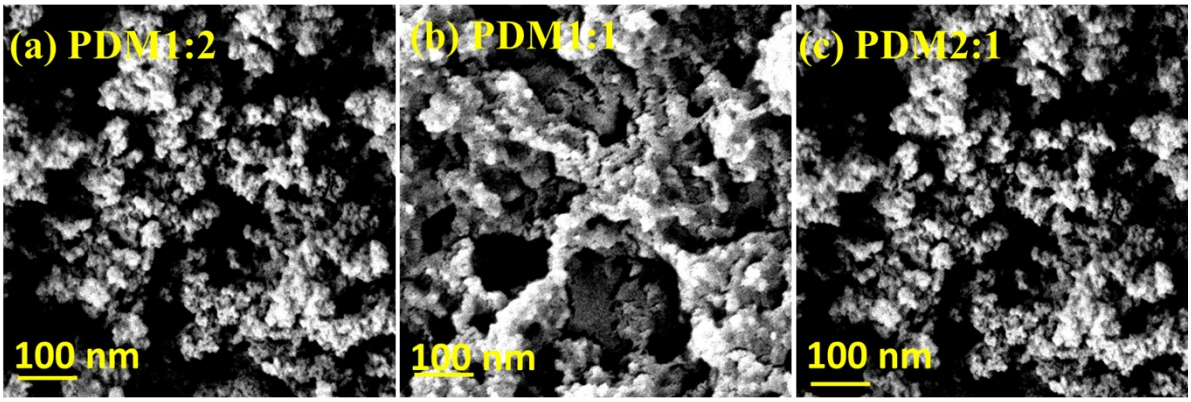

Fig. S13. *(a-c) FESEM images of post-chronoamperometric electrolysis electrodes, PDM1:2, PDM1:1, and PDM2:1, respectively.*

EIS fit results

Equivalent circuit: $R_1+Q_1/(R_2+C_3/R_3)$

R_1, R_2, and R_3 in the equivalent circuit diagram represent solution resistance, resistance due to PEDOT: PSS, and bulk resistance of the polymer, respectively. C_3 corresponds to double-layer capacitance, and Q_1 is constant phase element corresponding to the whole electrode-electrolyte layer.

Table S5. *R_1, Q_1, R_2, C_3 and R_3 values.*

Polymer	***R_1* (Ω)**	***Q_1* ($Fs^{1-\alpha}$)**	***R_2* (Ω)**	***C_3* (F)**	***R_3* (Ω)**
PDM2:1 Dark	20.5 ± 0.7	$6.1 \times 10^{-6} \pm 1.1 \times 10^{-7}$	10.8 ± 0.5	$8.9 \times 10^{-6} \pm 8.9 \times 10^{-8}$	22176±11.1
PDM2:1 Light	13.6 ± 0.4	$8.4 \times 10^{-6} \pm 3.8 \times 10^{-10}$	6.9 ± 0.3	$1.1 \times 10^{-5} \pm 1.2 \times 10^{-7}$	11704±25.3
PDM1:1 Dark	17.1 ± 2.1	$5.5 \times 10^{-5} \pm 3.9 \times 10^{-6}$	5.7 ± 2.6	$8.1 \times 10^{-6} \pm 5.2 \times 10^{-8}$	2105±26.5
PDM1:1 Light	32.2 ± 1.1	$3.1 \times 10^{-5} \pm 2.8 \times 10^{-6}$	4.4 ± 3.5	$3.7 \times 10^{-6} \pm 9.7 \times 10^{-7}$	960±3.9
PDM1:2 Dark	16.2 ± 0.6	$1.7 \times 10^{-5} \pm 6.9 \times 10^{-7}$	5.4 ± 1.2	$7.1 \times 10^{-6} \pm 3.1 \times 10^{-7}$	1073±3.3
PDM1:2 Light	17.1 ± 0.9	$2.2 \times 10^{-5} \pm 7.9 \times 10^{-6}$	5.1 ± 2.1	$5.7 \times 10^{-6} \pm 1.3 \times 10^{-6}$	549±14.8

Mott-Schottky results

Table S6. *M-S slope & U_{fb} values.*

Sample	M-S slope	U_{fb} (V)
PDM2:1	4.7×10^9	-0.92
PDM1:1	4.4×10^9	-1.05
PDM1:2	4.2×10^9	-1.12

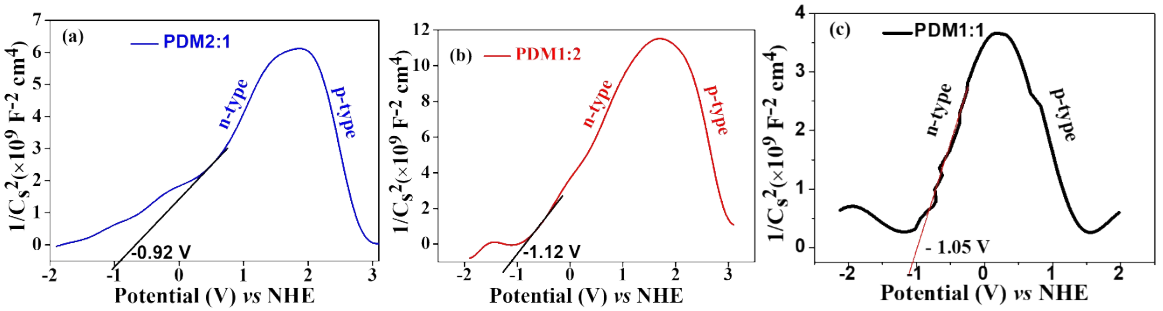

Fig. S14. ***(a-c)*** *Mott-Schottky plots of polymers PDM2:1, PDM1:2, and PDM1:1, respectively, showing both p-type and n-type semiconducting behavior.*

OWSR prototype video

OWS.mkv

Fig. S15. *Prototype showing overall water splitting (bulk electrolysis) under ambient light conditions using two AAA cells in series.*

References

[S1] S. Jayanthi, D. V. S. Muthu, N. Jayaraman, S. Sampath, A. K. Sood, *ChemistrySelect*. 2017, ***2***, 4522.

[S2] S. Roy, A. Bandyopadhyay, M. Das, P. P. Ray, S. K. Pati, T. K. Maji, *J. Mater. Chem. A Mater.* 2018, ***6***, 5587.

[S3] Y. Zhao, R. Nakamura, K. Kamiya, S. Nakanishi, K. Hashimoto, *Nat. Commun*. 2013, ***4***, 2390.

[S4] N. Cheng, Q. Liu, J. Tian, Y. Xue, A. M. Asiri, H. Jiang, Y. He, X. Sun, *Chem. Commun.* 2015, ***51***, 1616.

[S5] Y. Zhang, X. Fan, J. Jian, D. Yu, Z. Zhang, L. Dai, *Energy Environ. Sci.* 2017, ***10***, 2312.

[S6] A. Singh, S. Roy, C. Das, D. Samanta, T. K. Maji, *Chem. Commun.* 2018, ***54***, 4465.

[S7] Y. Liu, X. Guan, B. Huang, Q. Wei, Z. Xie, *Front. Chem.* 2020, ***7***, 805.

[S8] T. Ouyang, Y. Ye, C. Wu, K. Xiao, Z. Liu, *Angew. Chem.* 2019, ***131***, 4977.

[S9] T. Kumar, A. Karmakar, A. Halder, R. R. Koner, *Energy and Fuels.* 2022, ***36***, 2722.

[S10] X. Wang, A. Guo, Y. Fu, M. Tan, W. Luo, W. Yang, *ACS Appl. Nano. Mater.* 2023, ***6***, 3226.

[S11] N. Jiang, B. You, M. Sheng, Y. Sun, *Angew. Chem.* 2015, ***54***, 6251.

[S12] B. You, N. Jiang, M. Sheng, S. Gul, J. Yano, Y. Sun, *Chem. Mater.* 2015, ***27***, 7636.

[S13] C. C. L. McCrory, S. Jung, J. C. Peters, T. F. Jaramillo, *J. Am. Chem. Soc*. 2013, ***135***, 16977.

[S14] S. Mulkapuri, A. Ravi, R. Nasani, S. K. Kurapati, S. K. Das, *Inorg. Chem.* **2022**, *61*, 13868.

[S15] P. N. Singh, M. G. Mohamed, M. G. Kotp, T. Mondal, S. V. Chaganti, M. Ibrahim, S. U. Sharma, Y. Ye, S. W. Kuo, *ACS Appl. Polym. Mater.* 2025, ***7***, 3324-3336.

[S16] W. Guo, X. Luan, P. Sun, T. Wang, H. Luo, X. Li, C. Li, W. Tan, J. Bai, Q. Wang, B. Zhou, *Sustain. Energy Fuels* 2021, ***5***, 6085.

[S17] S. K. Das, A. Chowdhury, K. Bhunia, A. Ghosh, D. Chakraborty, M. Das, U. Kayal, A. Modak, D. Pradhan, A. Bhaumik, *Electrochim. Acta*. 2023, ***459***, 142553.

[S18] S. Sahoo, E. K. Johnson, X. Wei, S. Zhang, C. W. Machan, *Energy. Adv.* 2024, ***3***, 2280.

[S19] Y. Ito, W. Cong, T. Fujita, Z. Tang, M. Chen, *Angew. Chem*. 2015, ***54***, 2131.

[S20] Y. Ito, Y. Shen, D. Hojo, Y. Itagaki, T. Fujita, L. Chen, T. Aida, Z. Tang, T. Adschiri, M. Chen, *Adv. Mater.* 2016, ***28***, 10644.

[S21] Y. Zheng, Y. Jiao, Y. Zhu, L. H. Li, Y. Han, Y. Chen, A. Du, M. Jaroniec, S. Z. Qiao, *Nat. Commun.* 2014, ***5***, 3783.

[S22] L. Wei, H. E. Karahan, K. Goh, W. Jiang, D. Yu, Ö. Birer, R. Jiang, Y. Chen, *J. Mater. Chem. A.* 2015, ***3***, 7210.

[S23] D. Zhou, X. Tan, H. Wu, L. Tian, M. Li, *Angew. Chem.* 2019, ***131***, 1390.

[S24] T. Mondal, M. G. Mohamed, A. A. K. Mohamed, S. W. Kuo, *ACS Appl Energy Mater* 2025, ***8***, 7703.